Supporting Information

Study of Active Sites on Se-MnS/NiS Heterojunctions as Highly Efficient Bifunctional Electrocatalysts for Overall Water Splitting

Jie Zhu,[1] Mao Sun,[1] Shujie Liu,[1] Xianhu Liu,[2] Kan Hu,[1] and Lei Wang[1,2,*]

[1] College of Chemistry and Chemical Engineering, Inner Mongolia Key Lab of Nanoscience and Nanotechnology, Inner Mongolia University, Hohhot 010021, China

[2] Key Laboratory of Materials Processing and Mold, Ministry of Education, Zhengzhou University, Zhengzhou 450002, China

E-mail: wanglei@imu.edu.cn

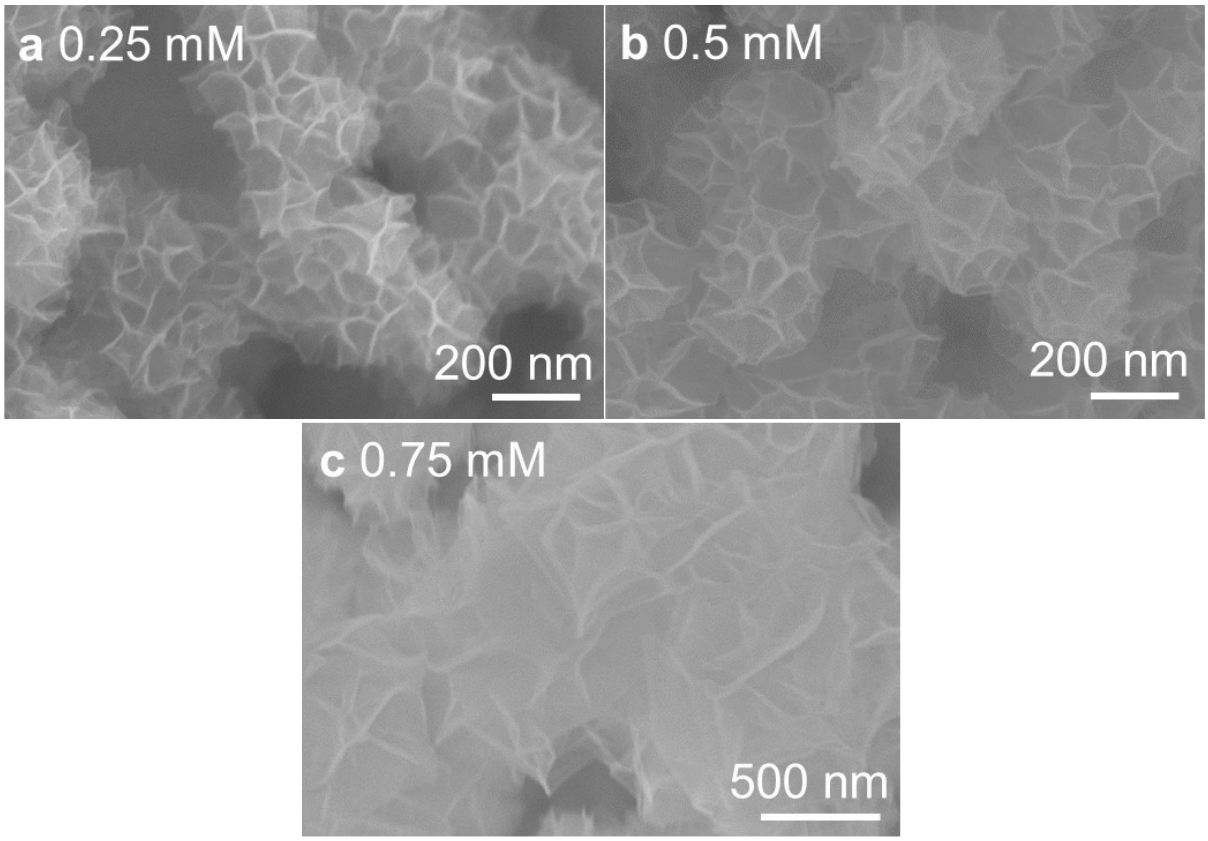

Figure S1. SEM images of NiMn LDH with various $KMnO_4$ concentrations: (a) 0.25 mM; (b) 0.5 mM; (c) 0.75 mM.

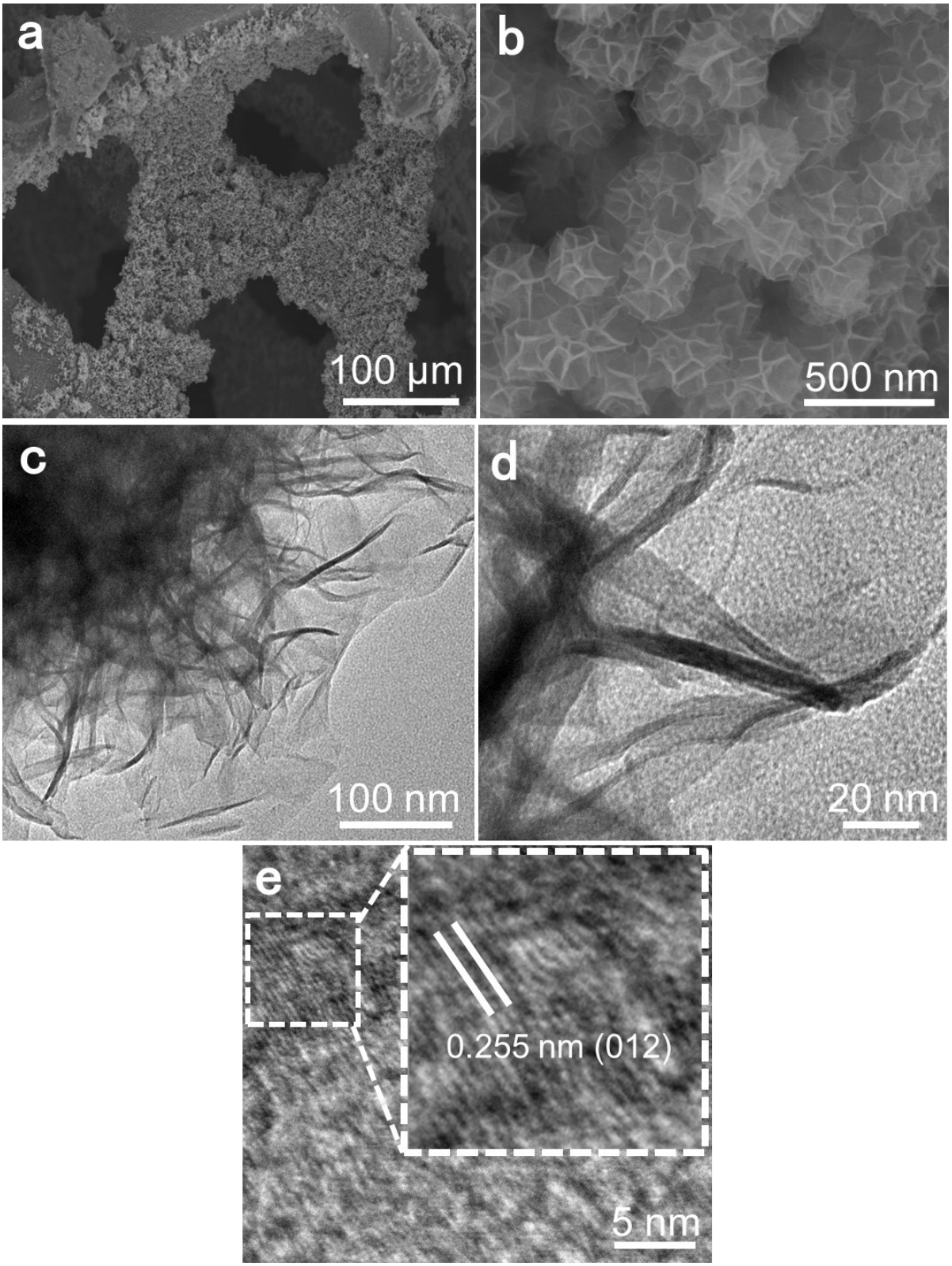

Figure S2. (a,b) SEM and (c-e) TEM images of NiMn LDH.

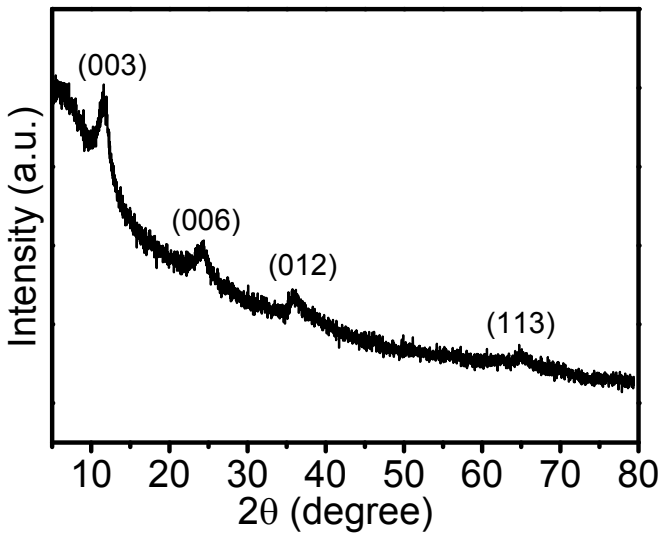

Figure S3. XRD pattern of NiMn LDH powder.

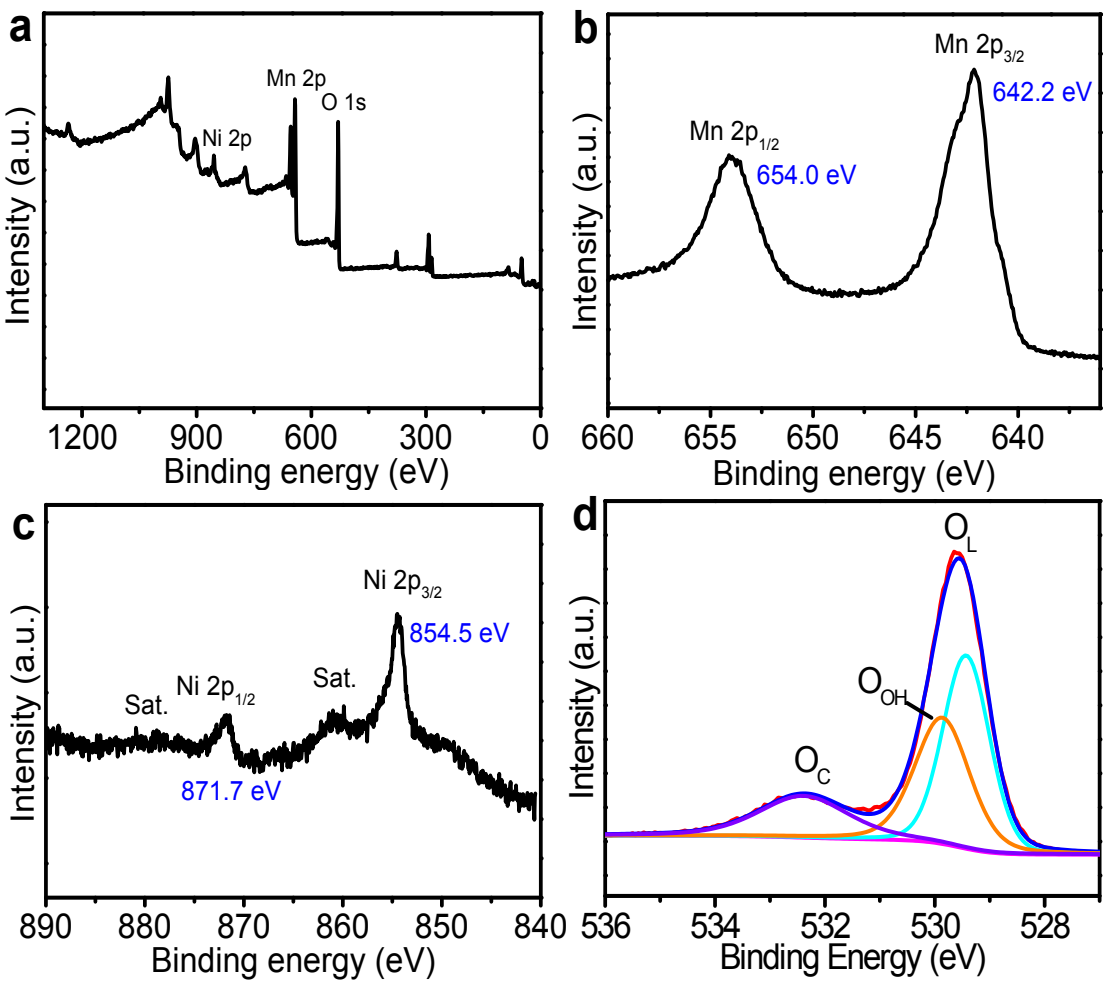

e

Element	wt.%	at.%
Mn	11.5	23.24
Ni	1.53	4.57
O	70.87	52.76

Figure S4. (a) XPS survey spectra, (b) Mn 2p, (c) Ni 2p, and (d) O 1s spectra of NiMn LDH; (e) corresponding element contents. Mn 2p spectrum indicates the 4+ oxidation state of Mn in LDH.

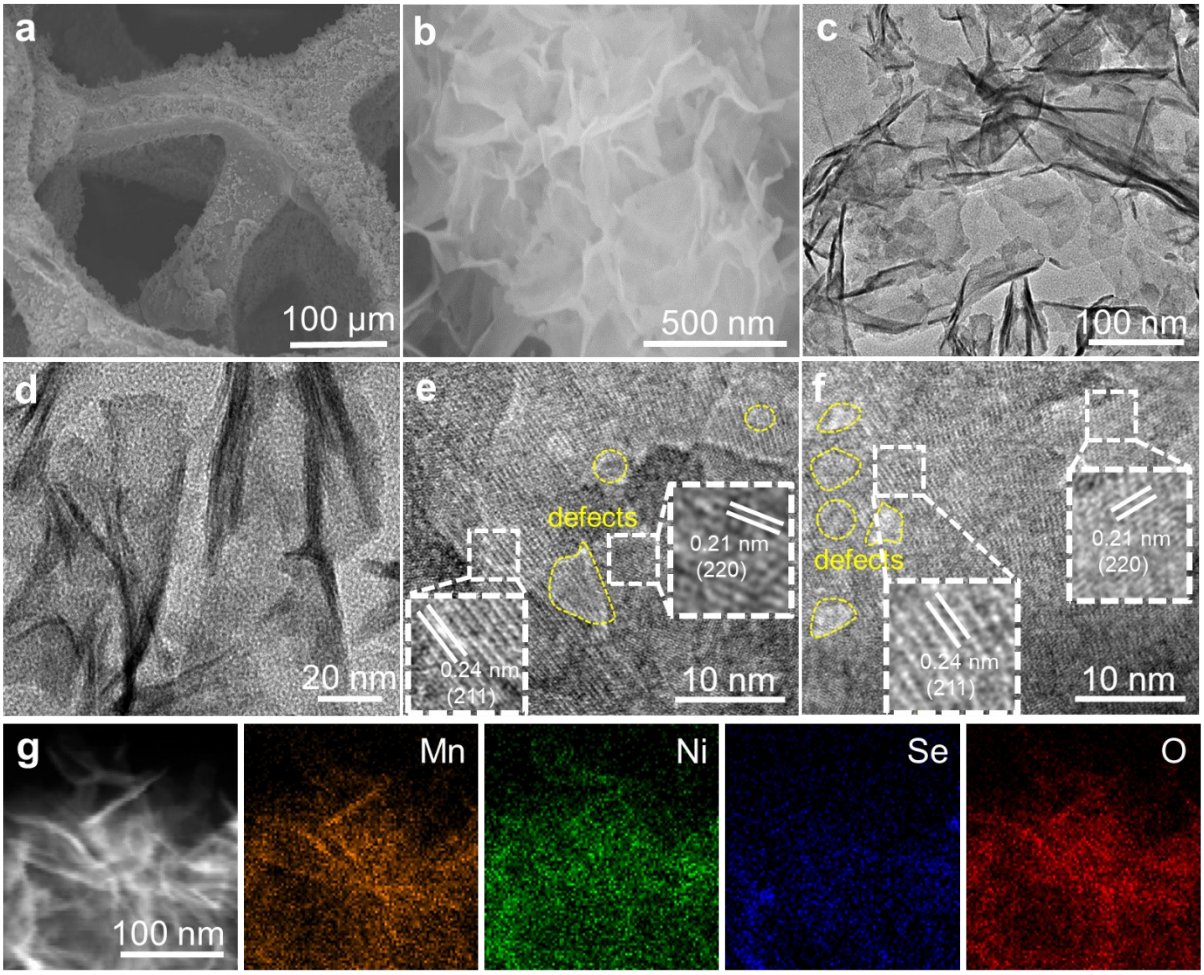

Figure S5. (a,b) SEM, (c-f) TEM images, and (g) EDS mappings of Se-NiMn oxide. It shows the homogeneous distribution of Mn, Ni, Se, and O.

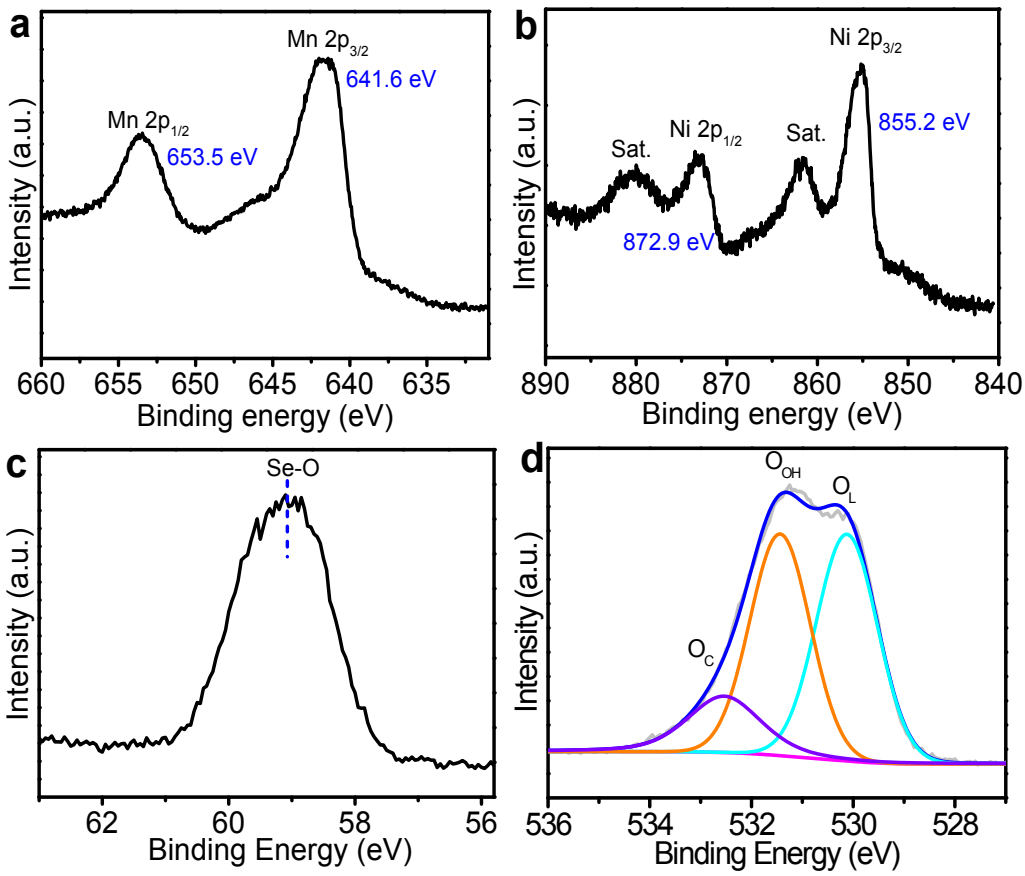

e

Element	wt.%	at.%
Mn	9.24	18.31
Ni	3.17	9.3
Se	11.04	6.83
O	52.49	53.19

Figure S6. (a) Mn 2p, (b) Ni 2p, (c) Se 3d, and (d) O 1s XPS spectra of Se-NiMn oxide; (e) corresponding element contents.

The lattice defects and amorphous phase existed in Se-NiMn oxide can be attributed to the incorporation of Se. The nanosheet structure of Se-NiMn oxide becomes thinner compared to the NiMn LDH. Besides, after selenization, Se 3d XPS peak (**Figure S6c**) shows the Se-O bond, while no metal-Se bond is formed, indicating the incorporation of Se in the host material. The O 1s XPS peak (**Figure S6d**) exhibits the obvious hydroxyl oxygen -OH bond in Se-NiMn oxide compared to that of NiMn LDH. This provides an information that the hydroxylated

surface of Se-NiMn oxide after selenization owing to the Se doping. These results are in accordance with the literature as well.[1]

[1] C. Hu, L. Zhang, Z.-J. Zhao, A. Li, X. Chang and J. Gong, *Adv. Mater.*, 2018, **30**, 1705538.

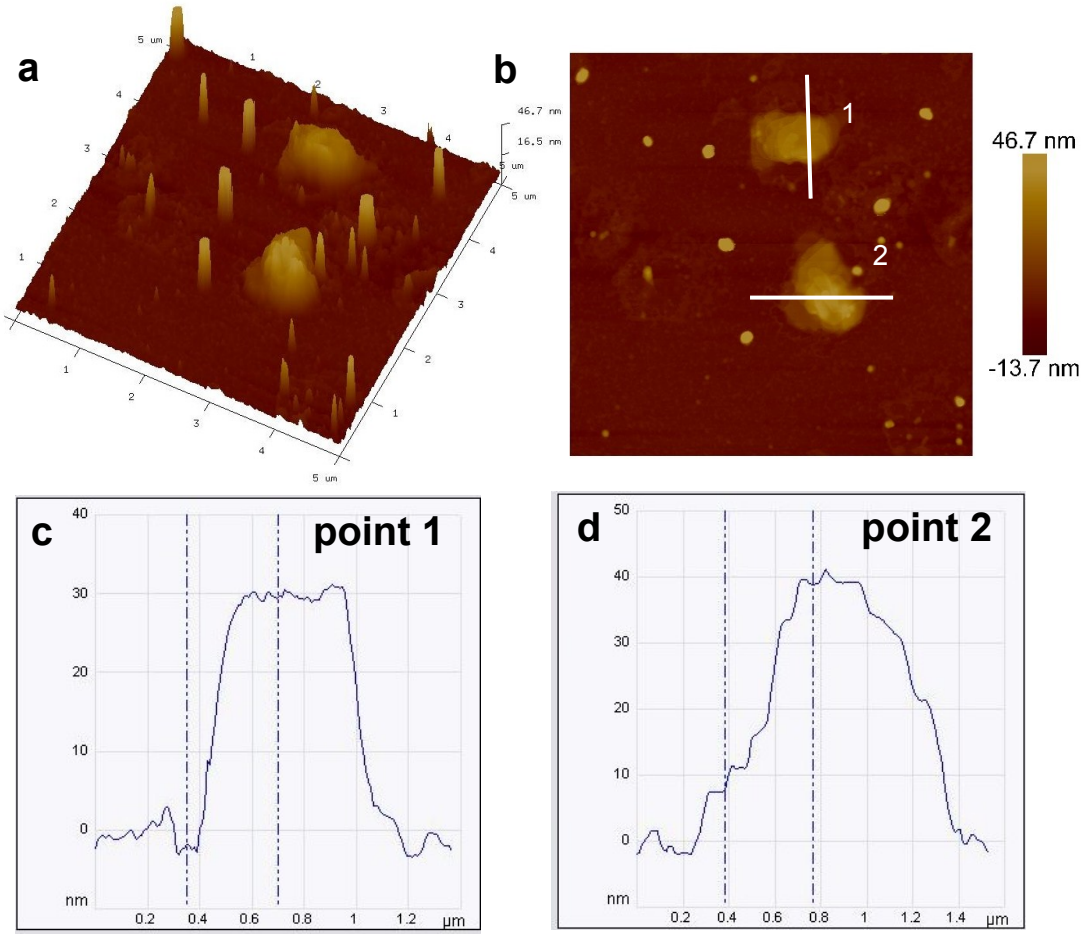

Figure S7. (a,b) AFM images and (c,d) corresponding line scan profiles of Se-MnS/NiS.

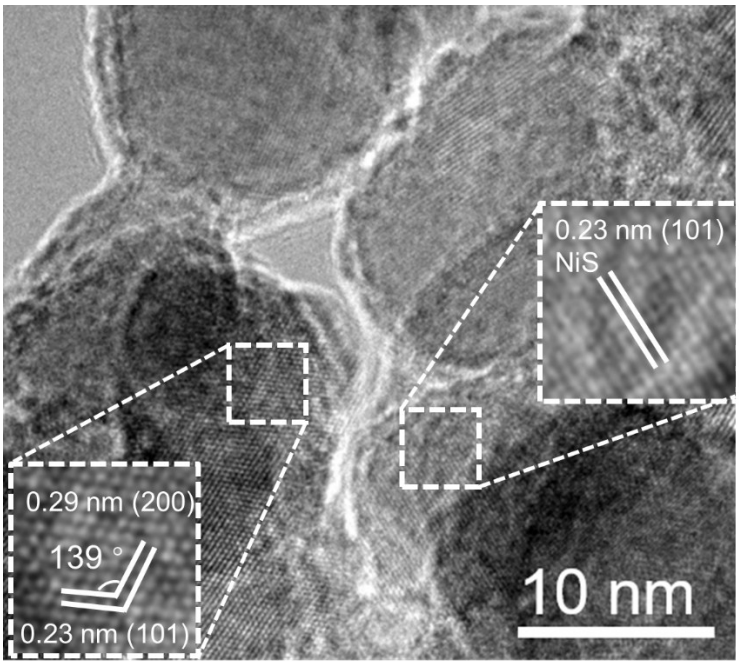

Figure S8. TEM image of Se-MnS/NiS heterostructure.

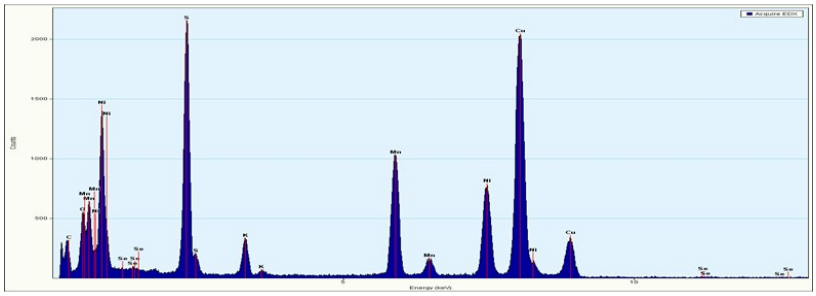

Element	wt.%	at.%
Mn	30.74	21.05
Ni	25.86	16.57
Se	0.19	0.09
S	33.37	39.17
O	9.82	23.10

Figure S9. TEM-EDS spectrum of Se-MnS/NiS with the corresponding element contents.

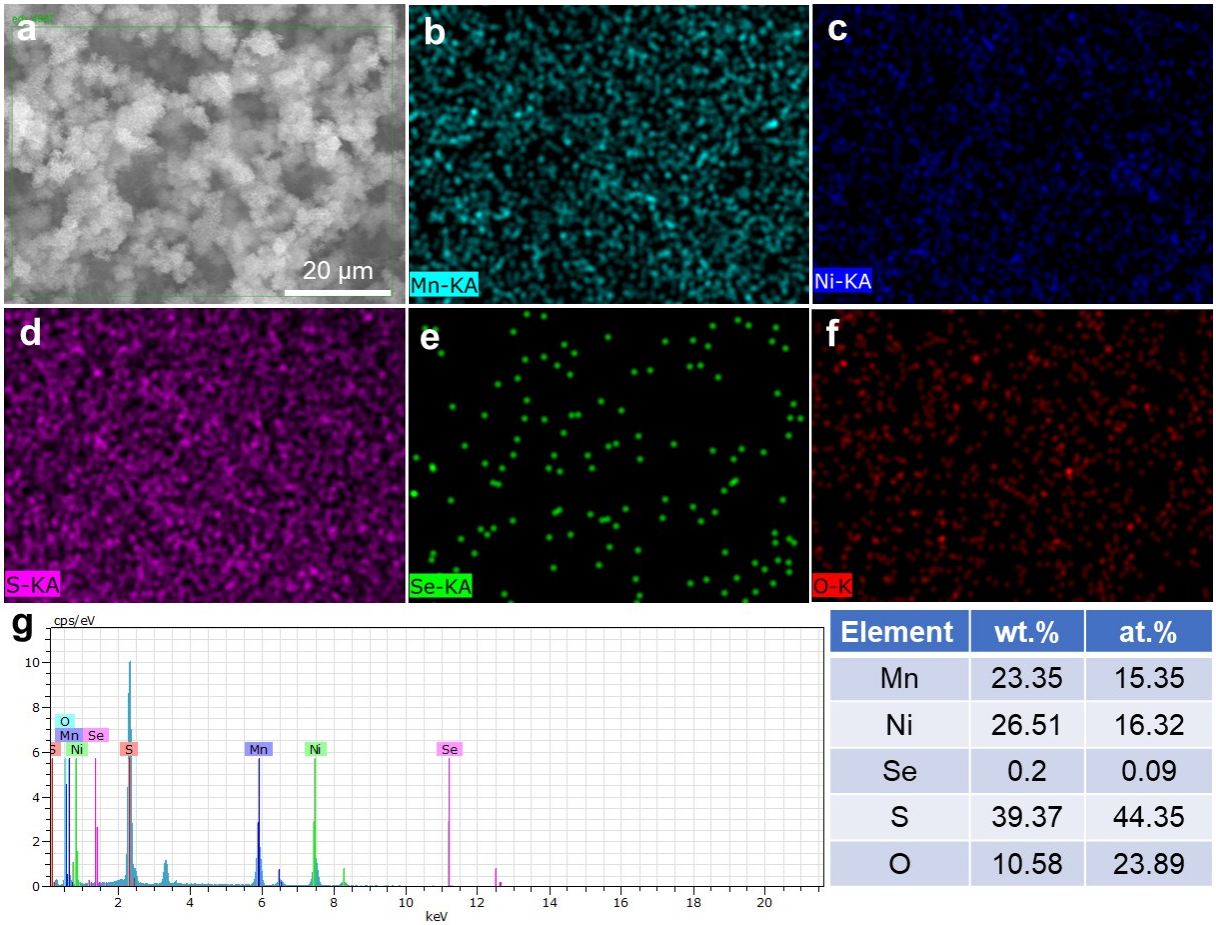

Element	wt.%	at.%
Mn	23.35	15.35
Ni	26.51	16.32
Se	0.2	0.09
S	39.37	44.35
O	10.58	23.89

Figure S10. (a) SEM image of Se-MnS/NiS and corresponding element mappings of (b) Mn, (c) Ni, (d) S, (e) Se, and (f) O; (g) EDX spectrum of Se-MnS/NiS with the corresponding element contents.

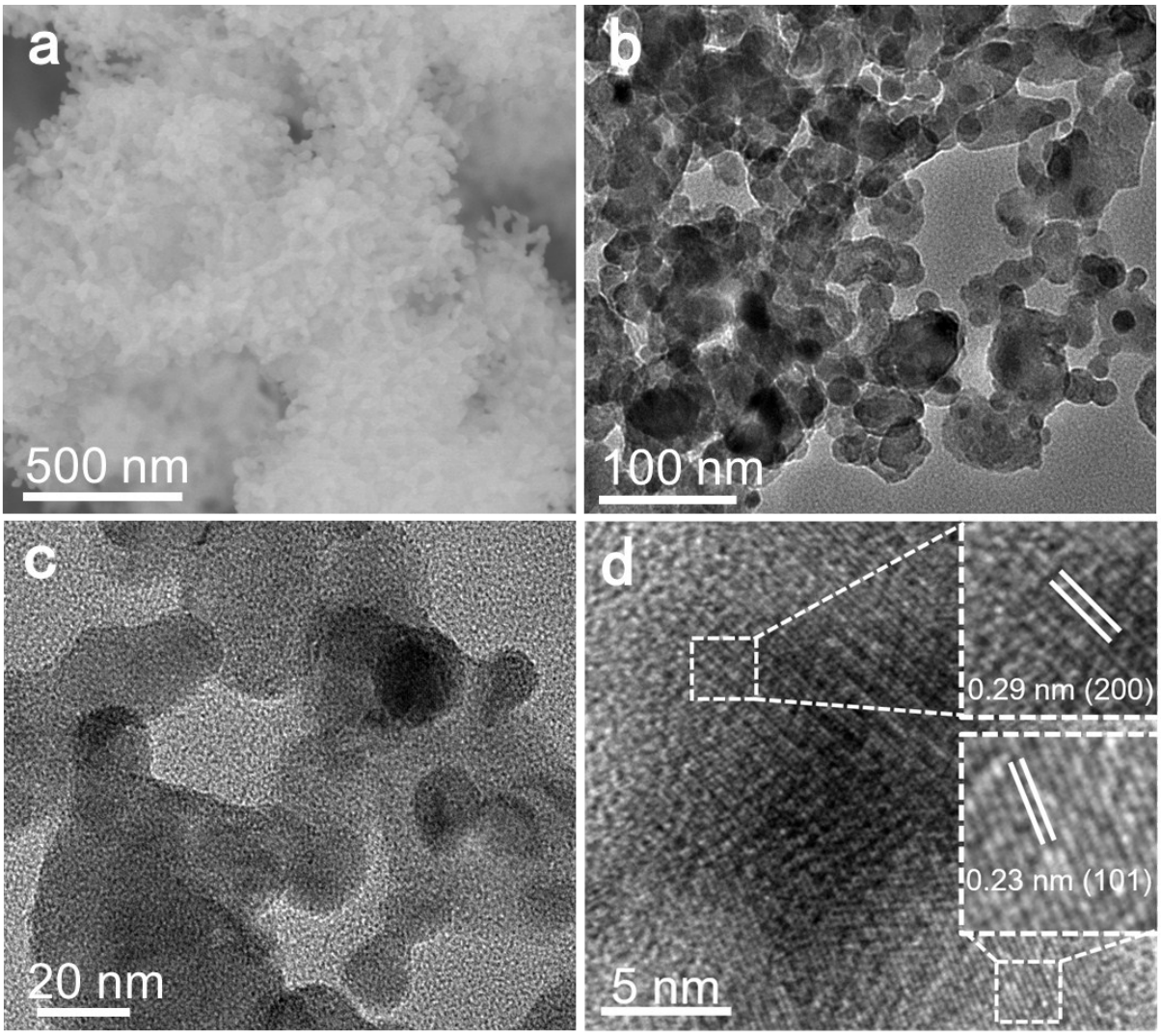

Figure S11. TEM images of MnS/NiS.

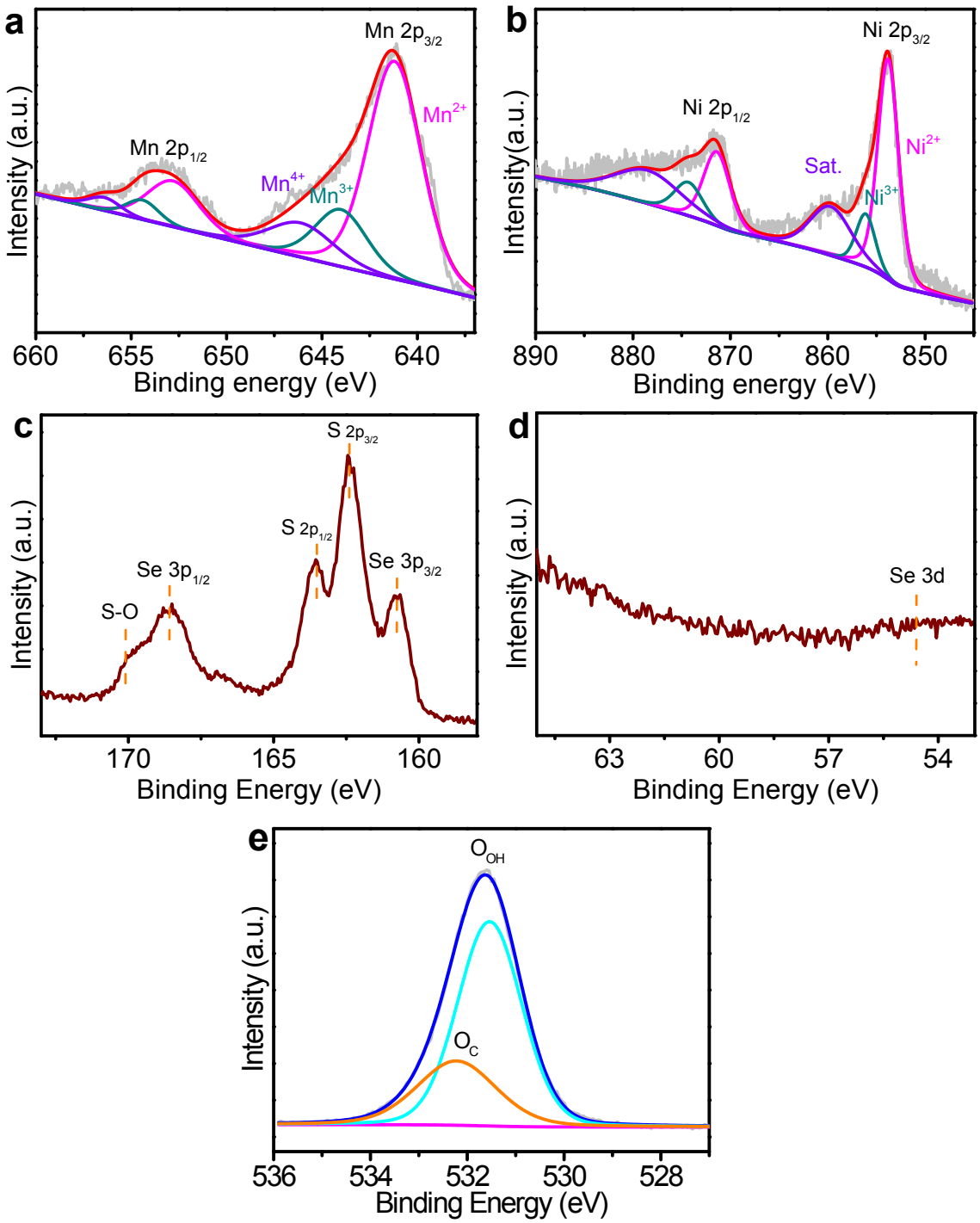

Figure S12. (a) Mn 2p, (b) Ni 2p, (c) S 2p and Se 3p, (d) Se 3d, and (e) O 1s XPS spectra of Se-MnS/NiS.

In the O 1s spectrum (**Figure S12e**), the peak at 531.7 eV attributed to hydroxyl oxygen -OH bond is shown on the Se-MnS/NiS. The amorphous layer with a thickness of 1-2 nm is hydroxide covered on the top surface.

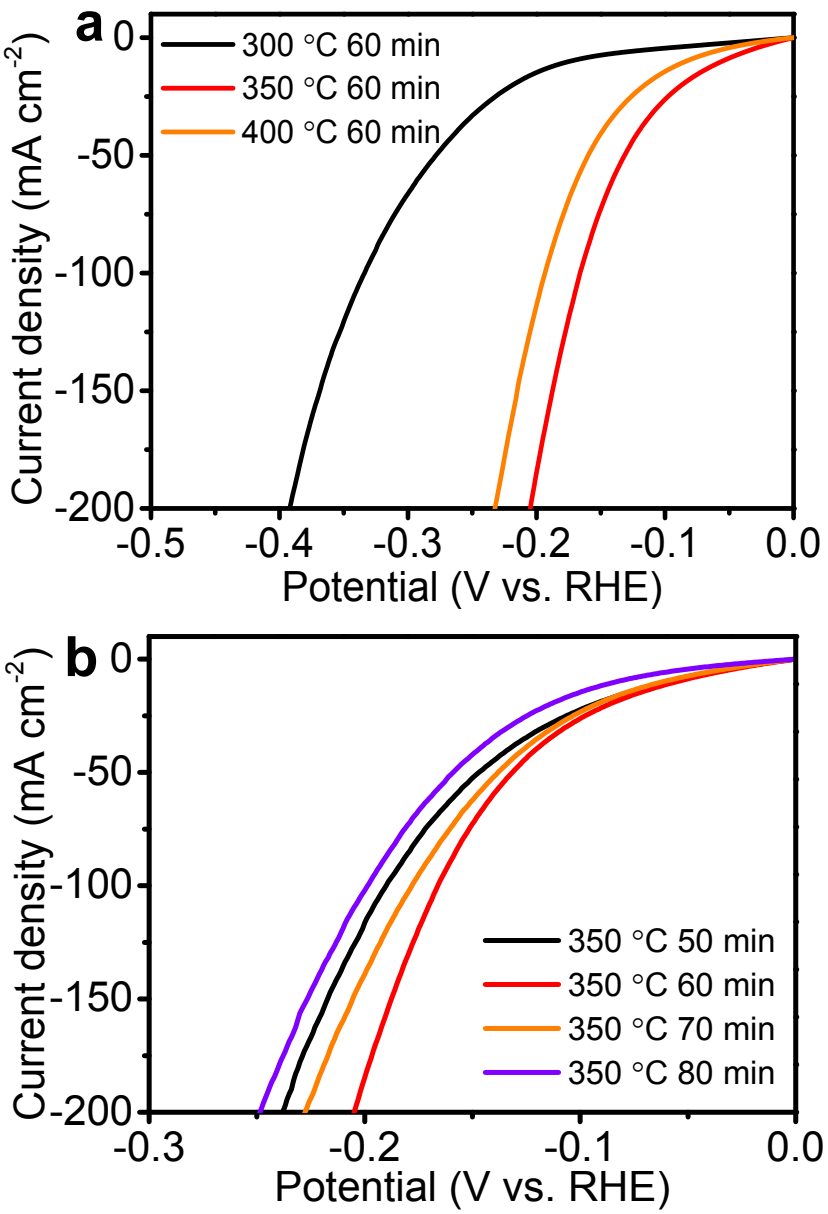

Figure S13. IR-corrected LSV curves for HER of Se-MnS/NiS with different S annealing temperatures (a) and times (b) in 1 M KOH. The optimal sulfuration time for HER is at 350 °C for 60 min.

Table S1. The HER performances of different catalysts in 1 M KOH electrolyte.

Catalysts	η_{10} (mV)	Tafel slope (mV dec^{-1})	J_0 (mA cm^{-2})
Se-MnS/NiS	56	55	967
MnS/NiS	92	111	664
NiMn LDH	220	128	298
NF	250	150	178
Pt/C	46	41	1198

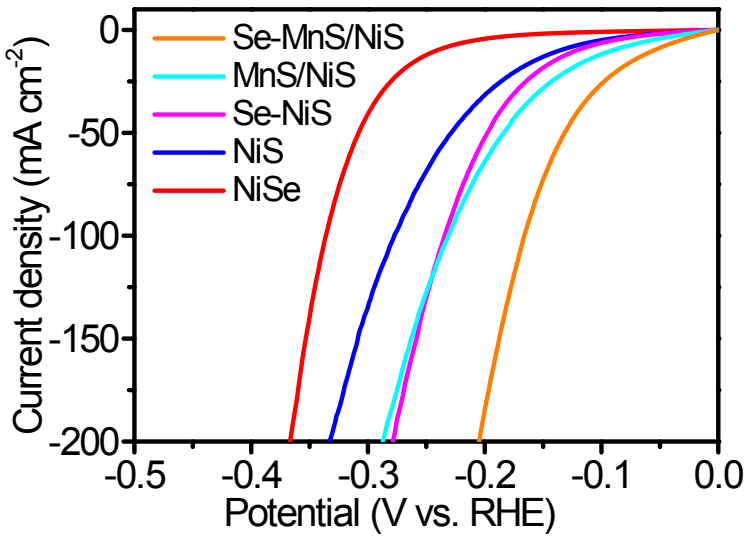

Figure S14. IR-corrected LSV curves for HER of NiSe, NiS, Se-NiS, MnS/NiS, and Se-MnS/NiS in 1 M KOH.

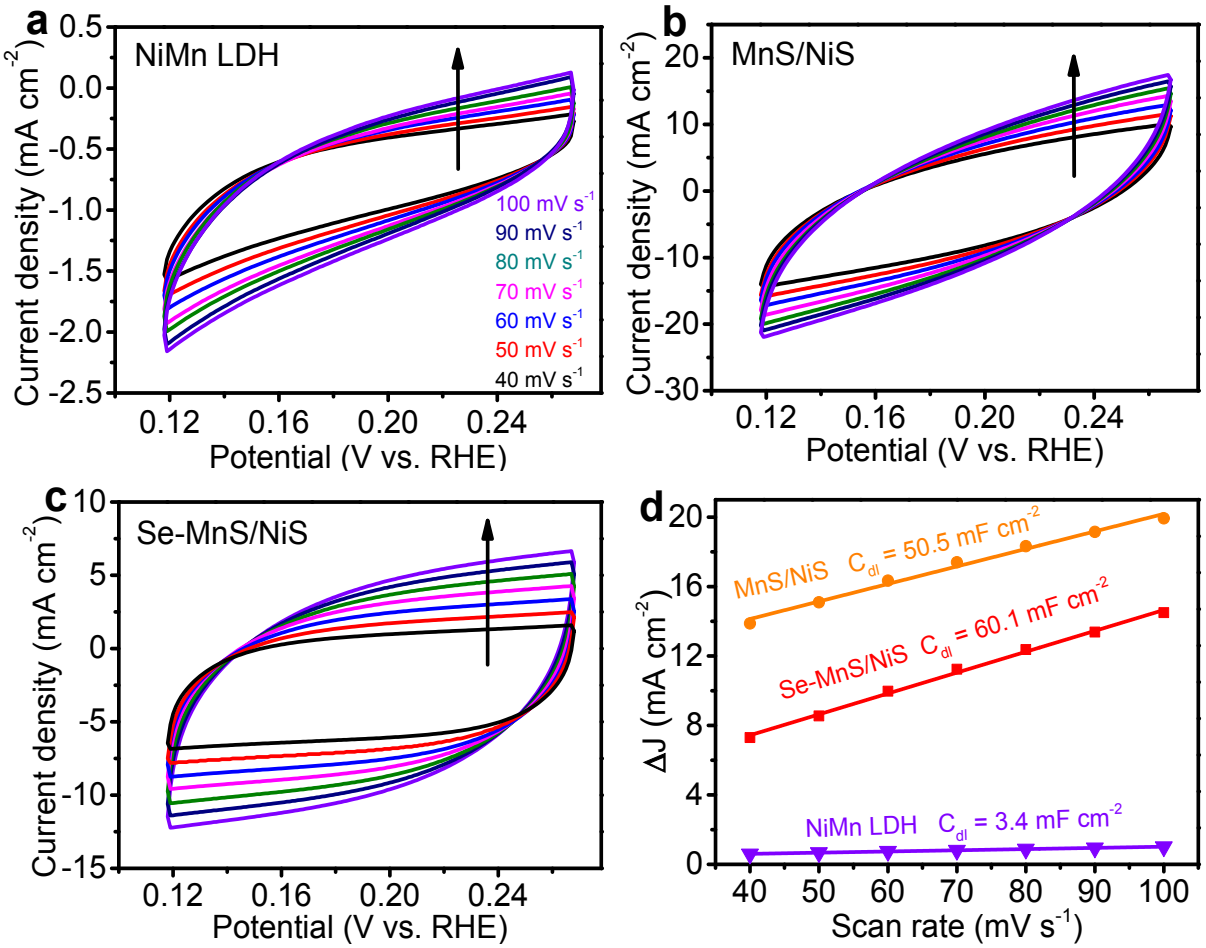

Figure S15. (a-c) CV curves of (a) NiMn LDH, (b) MnS/NiS, and (c) Se-MnS/NiS for HER at different scan rates; (d) liner fitting of the C_{dl} of the catalysts versus scan rate for the estimation of the ECSA.

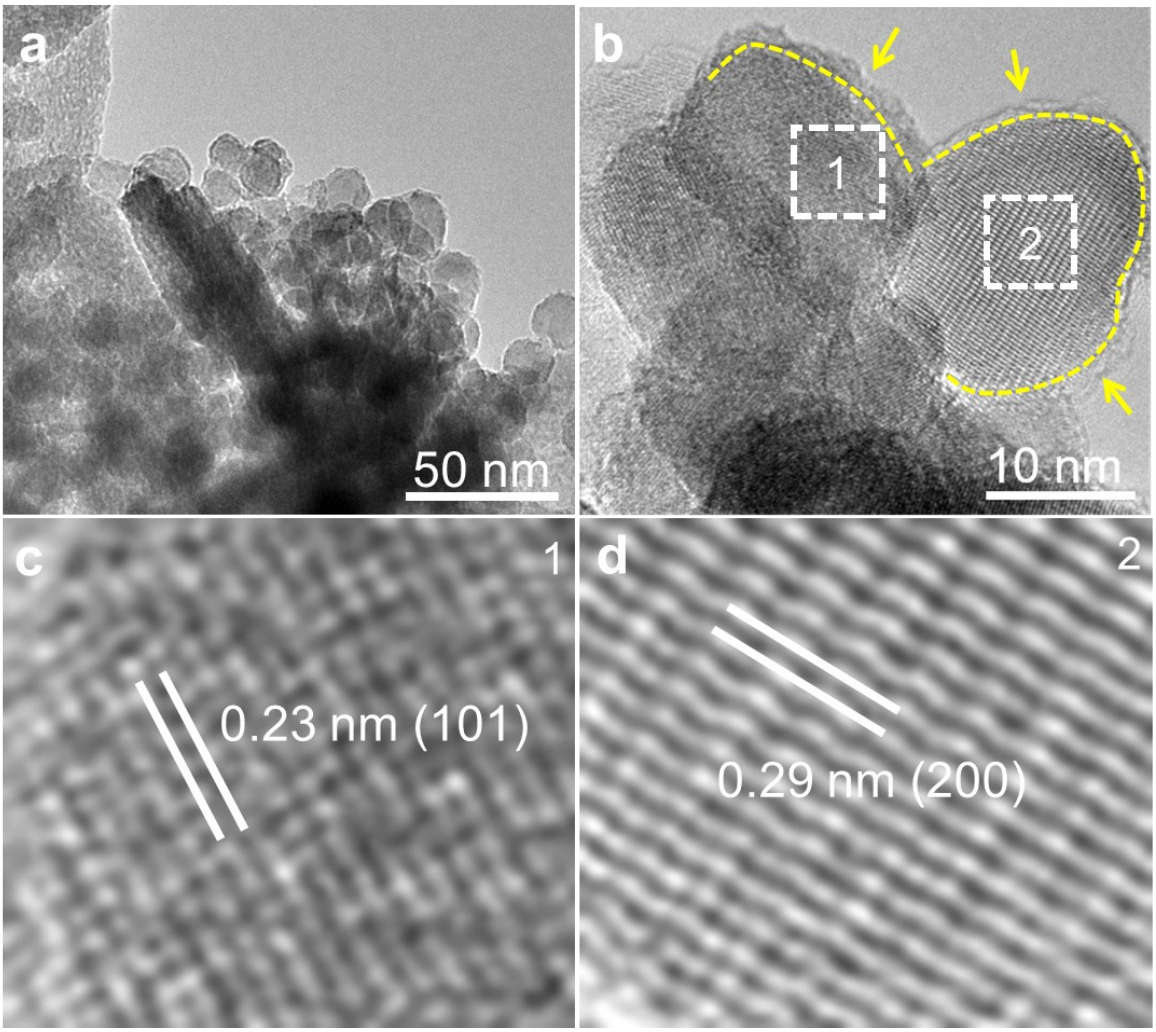

Figure S16. TEM images of Se-MnS/NiS after HER.

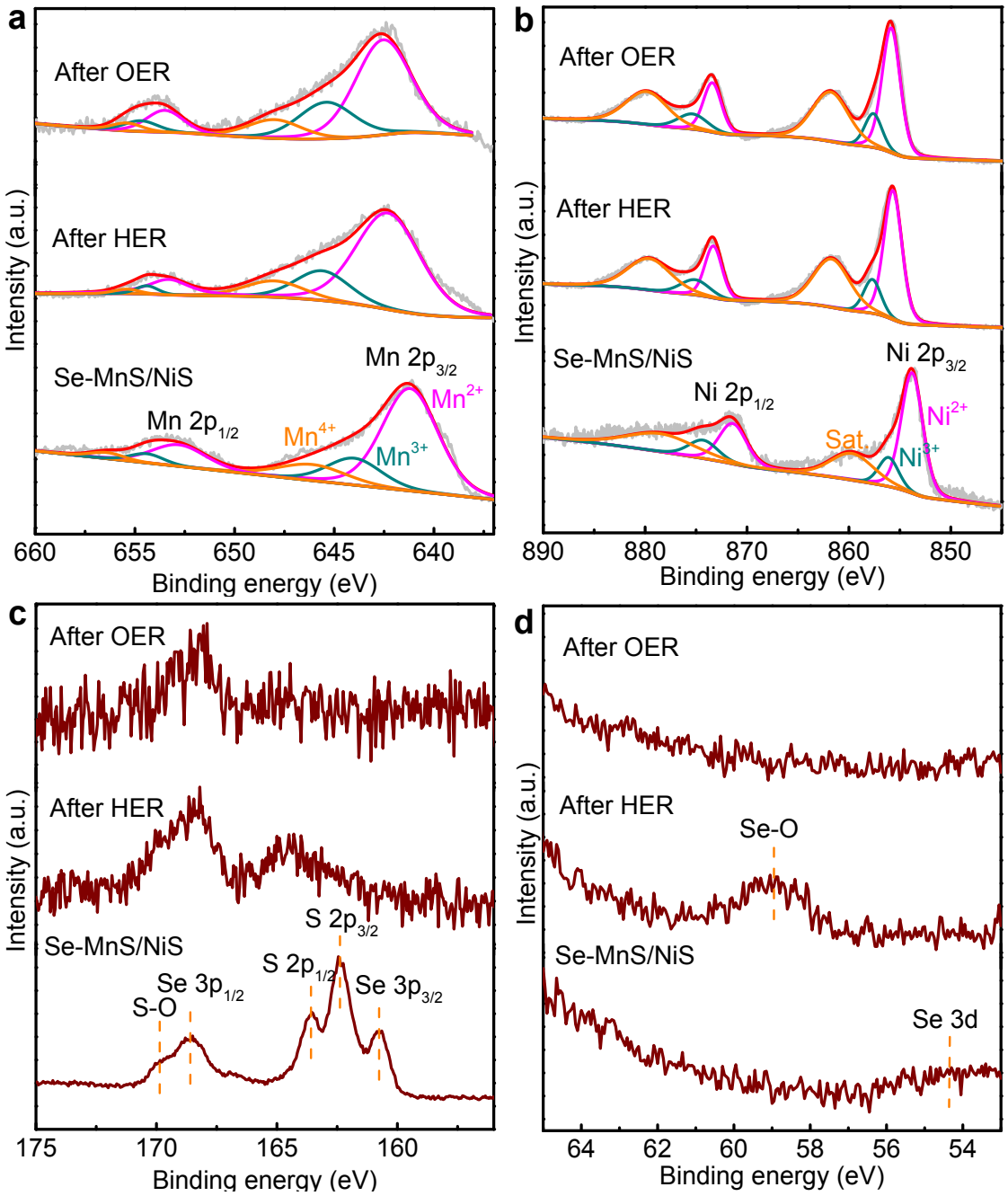

Figure S17. (a) Mn 2p, (b) Ni 2p, (c) S 2p, and (d) Se 3d XPS spectra of Se-MnS/NiS before and after HER and OER.

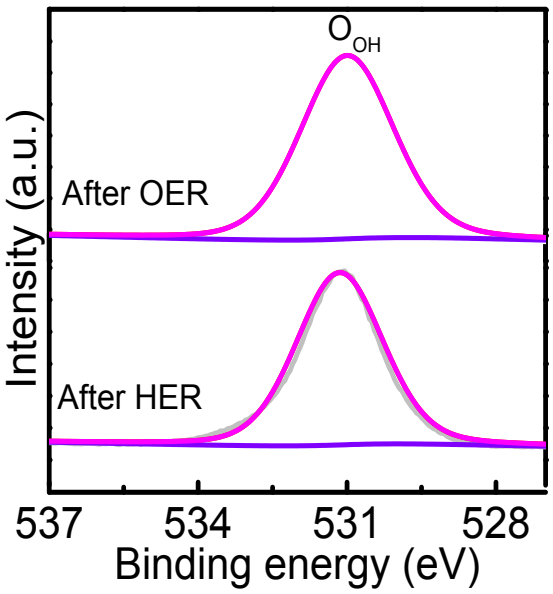

Figure S18. O 1s XPS spectra of Se-MnS/NiS after HER and OER.

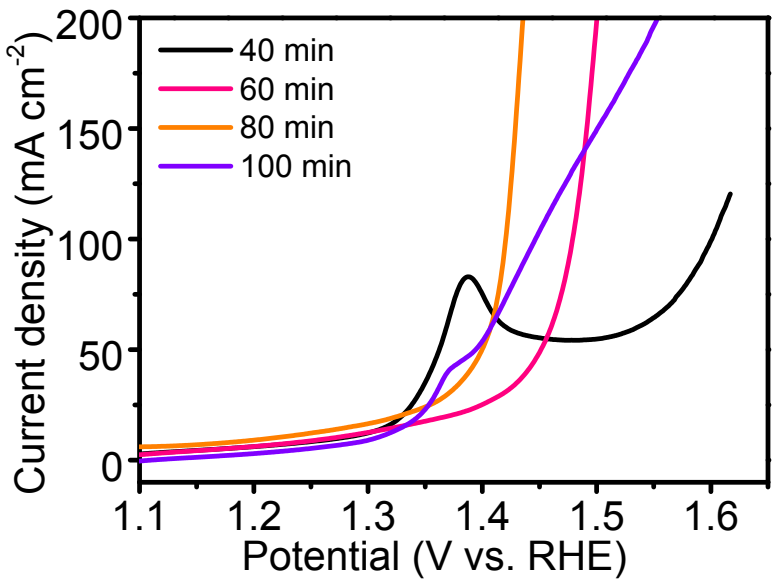

Figure S19. IR-corrected LSV curves for OER of Se-MnS/NiS with different S annealing times at 350 °C in 1 M KOH. The optimal sulfuration time for OER is 80 min.

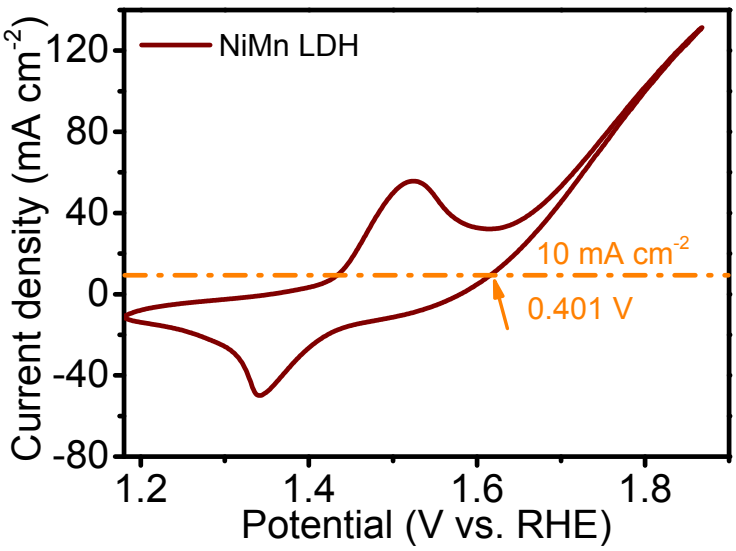

Figure S20. Determination of overpotential for OER by cyclic voltammetry at a scan rate of 50 mV s^{-1}. Here take NiMn LDH catalyst as example.

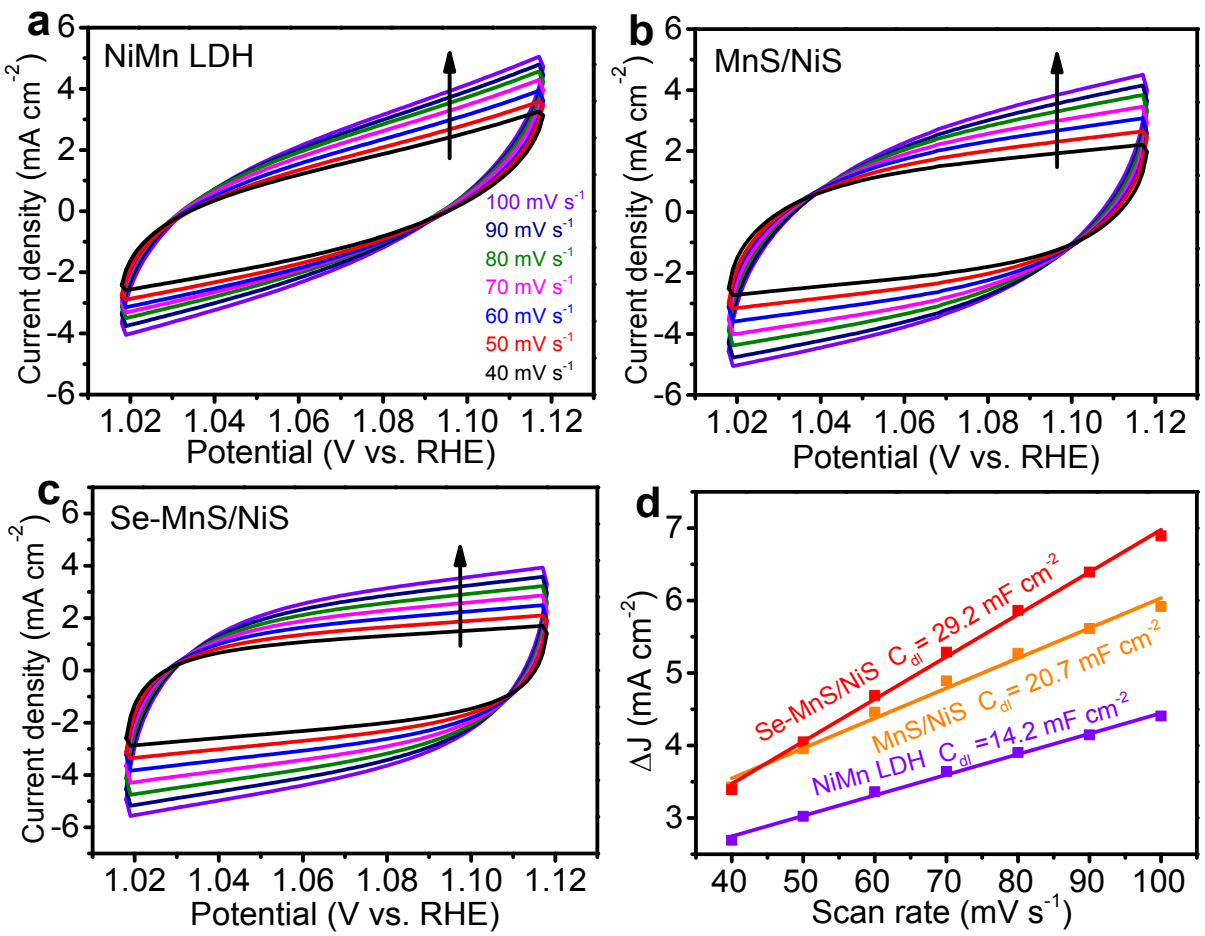

Figure S21. (a-c) CV curves of (a) NiMn LDH, (b) MnS/NiS and (c) Se-MnS/NiS for OER at different scan rates; (d) liner fitting of the C_{dl} of the catalysts versus scan rate for the estimation of the ECSA.

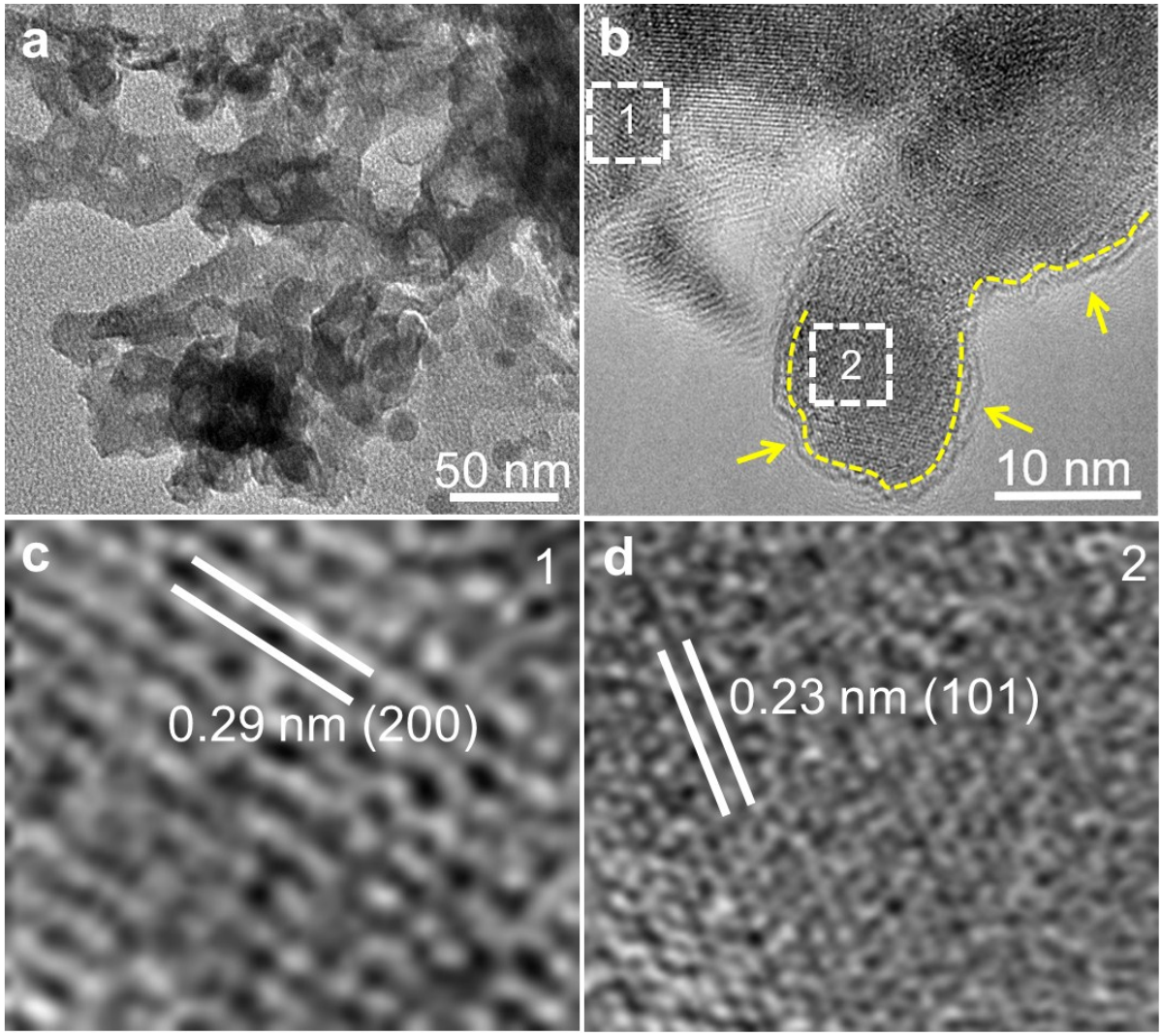

Figure S22. TEM images of Se-MnS/NiS after OER.

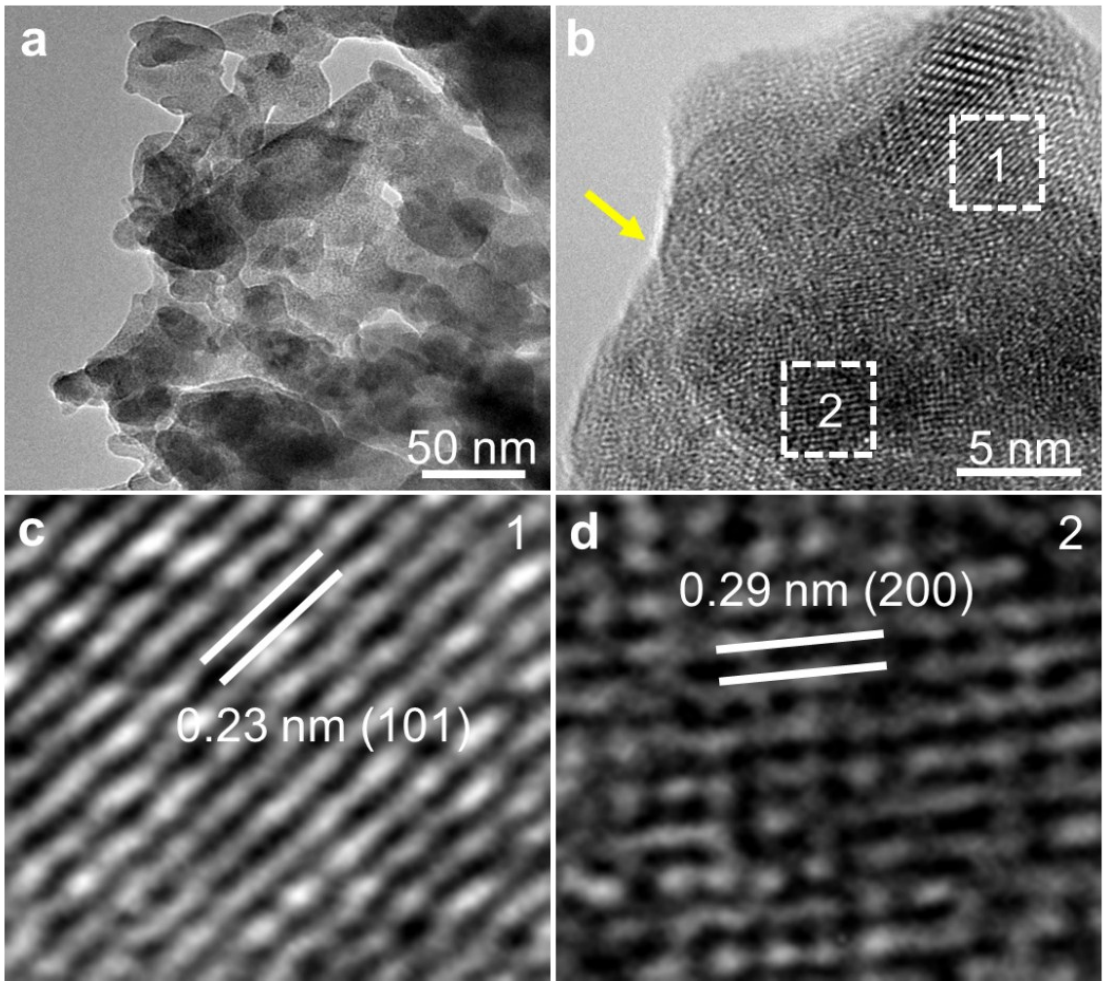

Figure S23. TEM images of Se-MnS/NiS after Ar plasma etching. The samples were treated in Ar plasma condition at 200 W for 20 min.

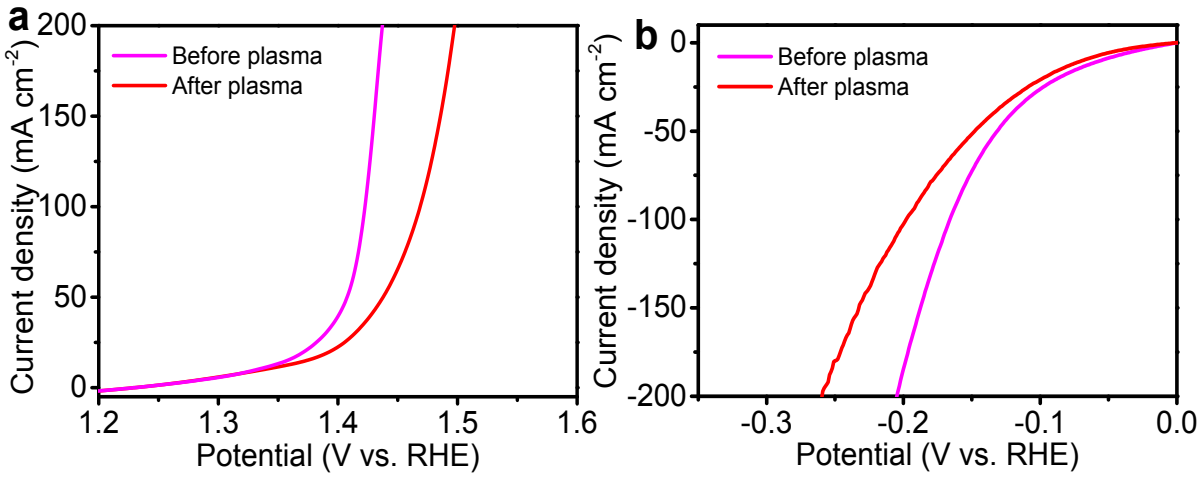

Figure S24. IR-corrected LSV curves for (a) OER and (b) HER of Se-MnS/NiS with and without the amorphous layer.

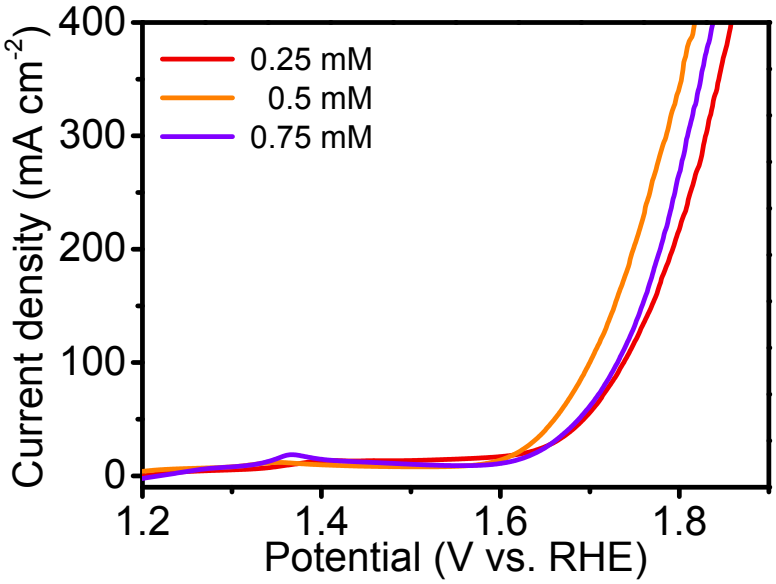

Figure S25. IR-corrected LSV curves for OER of NiMn LDH with different $KMnO_4$ concentrations in 1 M KOH.

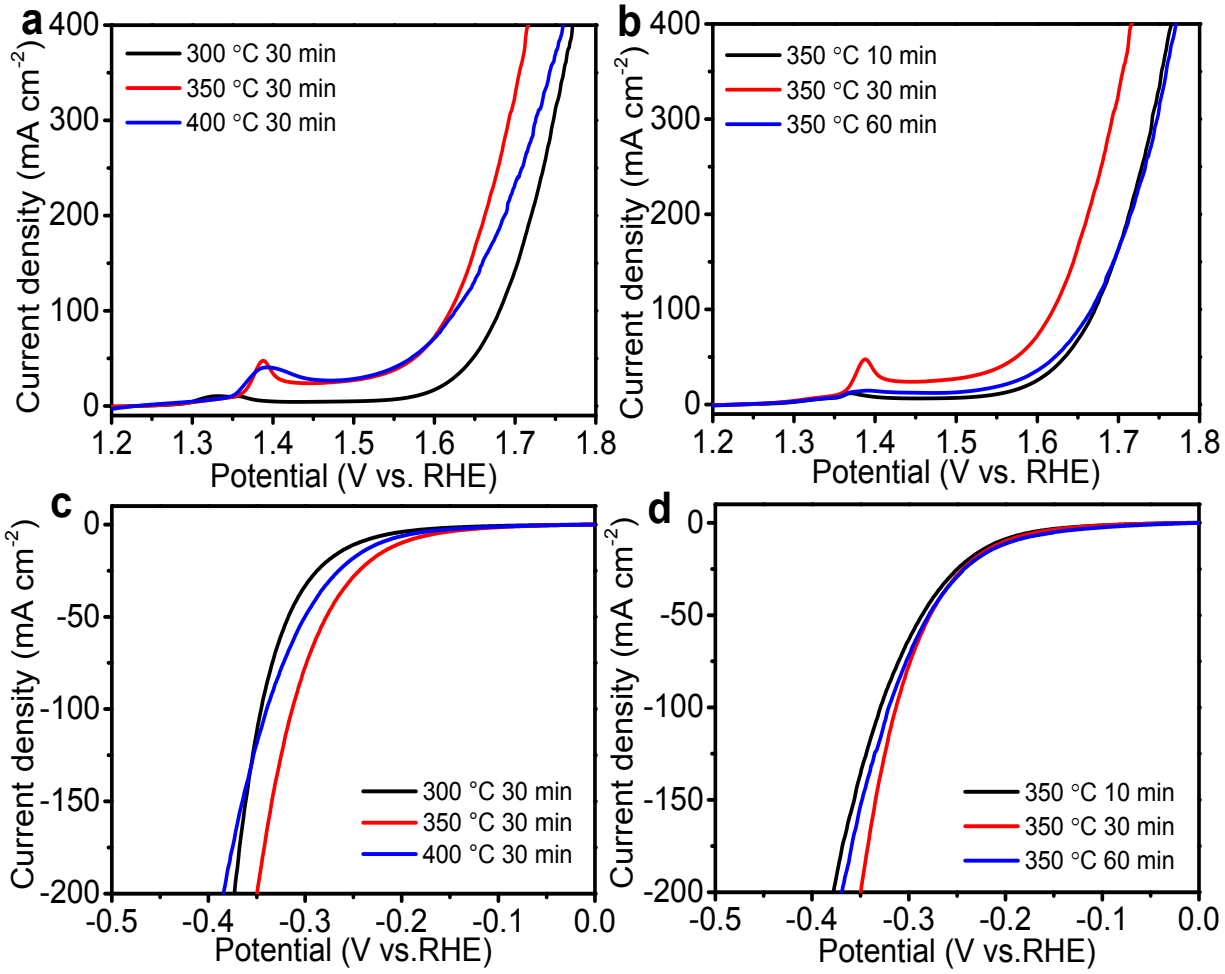

Figure S26. IR-corrected LSV curves for OER (a,b) and HER (c,d) of Se-NiMn oxide with different Se annealing temperatures (a,c) and times (b,d) in 1 M KOH. The optimal sulfuration time for OER and HER is 350 °C for 30 min.

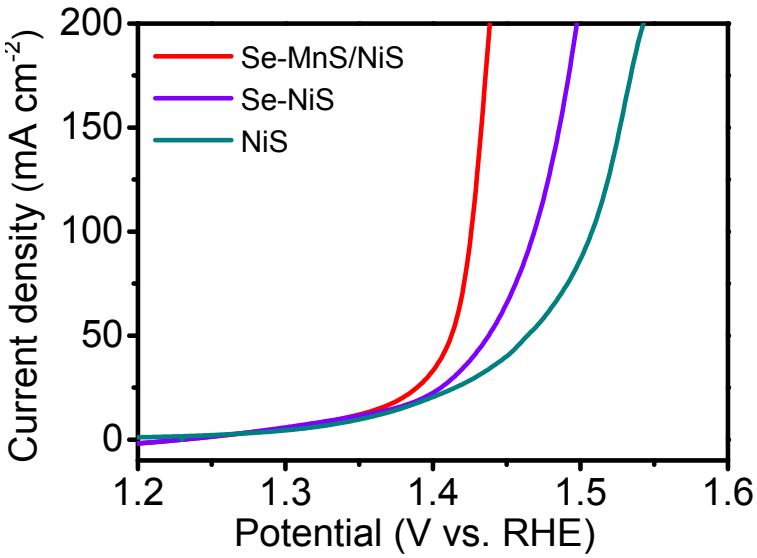

Figure S27. IR-corrected LSV curves for OER of NiSe, NiS, Se-NiS, MnS/NiS, and Se-MnS/NiS in 1 M KOH.

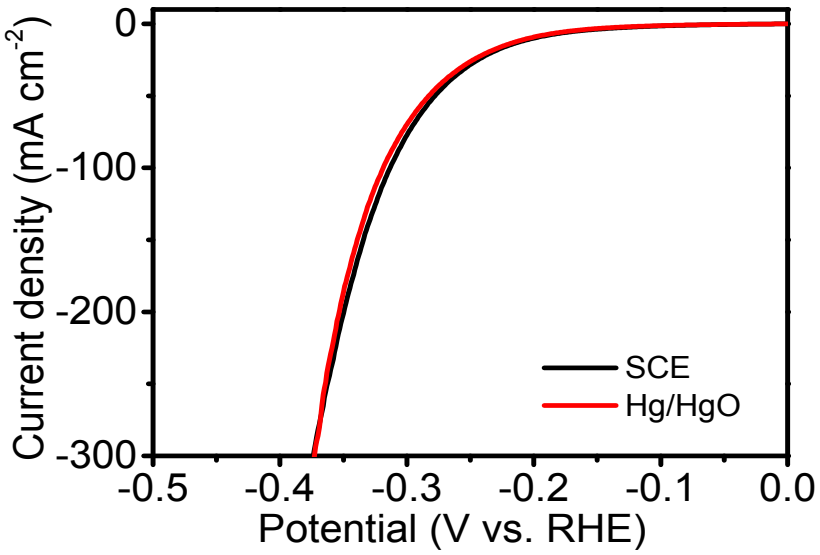

Figure S28. Comparison of HER performance in 1 M KOH under different reference electrodes. Here take NiMn LDH as example.

Please note：E (vs. RHE) = E (vs. SCE) + 0.0591×pH + 0.2412 (25 ℃)

E (vs. RHE) = E (vs. Hg/HgO) + 0.0591×pH + 0.098 (25 ℃)

Table S2. Comparison of the HER performance of Se-MnS/NiS with other recently reported electrocatalysts in 1 M KOH.

Catalyst	Electrolyte	Substrate	η_{10} (mV)	Tafel slope (mV dec^{-1})	Stability (h)	Reference
Se-MnS/NiS	1M KOH	Ni foam	56	55	48	This work.
Ni_3N-VN/NF	1M KOH	Ni foam	64	37	20	1
NF/T(Ni_3S_2/MnS-O)	1M KOH	Ni foam	116	41	50	2
Fe_3W_3C NRs/RGO	1M KOH	Glassy carbon	77	80	10^4 cycles	3
Co@N-CS/N-HCP@CC	1M KOH	Carbon cloth	66	65	30	4
Co_3S_4/EC-MOF	1M KOH	Carbon cloth	84	82	24	5
NF-Ni_3S_2/MnO_2	1M KOH	Ni foam	102	69	48	6
Co_9S_8/Ni_3S_2	1M KOH	Ni foam	128	97.6	9	7
Cu-Ni nanocages	1M KOH	Glassy carbon	140	79	8	8
N-Co_2P/CC	1M KOH	Carbon cloth	34	51	3.3	9
Se- (NiCo)S/OH	1M KOH	Ni foam	103	87.3	80	10
NiFe LDH@NiCoP/NF	1M KOH	Ni foam	120	88.2	100	11

References

1. H. J. Yan, Y. Xie, A. P. Wu, Z. C. Cai, L. Wang, C. G. Tian, X. M. Zhang and H. G. Fu, *Adv. Mater.*, 2019, **31**, 1901174.
2. Y. Zhang, J. L. Fu, H. Zhao, R. J. Jiang, F, Tian and R. J. Zhang, *Appl. Catal. B: Environ.,* 2019,

257, 117899.

3. C. Y. He, T. Bo, B. T. Wang and J. Z. Tao, *Nano Energy,* 2019, **62**, 85-93.
4. Z. L. Chen, Y. Ha, H. X. Jia, X. X. Yan, M. C, M. Liu and R. B. Wu, *Adv. Energy Mater*., 2019, **9**, 1803918.
5. T. Liu, P. Li, N. Yao, T. G. Kong, G. Z. Cheng, S. L. Chen and W. Luo, *Adv. Mater.,* 2019, **31**, 1806672.
6. Y. Xiong, L. L. Xu, C. D. Jin and Q. F. Sun, *Appl. Catal. B: Environ.,* 2019, **254**, 329-338.
7. F. Du, L. Shi, Y. T. Zhang, T. Li, J. L. Wang, G. H. Wen, A. Alsaedi, T. Hayat, Y. Zhou and Z. G. Zou, *Appl. Catal. B: Environ.,* 2019, **253**, 246-252.
8. Z. X. Li, C. C. Yu, Y. Y. Wen, Y. Gao, X. F. Xing, Z. T. Wei, H. Sun, Y. W. Zhang and W. Y. Song, *ACS Catal.,* 2019, **9**, 5084-5095.
9. Y. N. Men, P. Li, J. H. Zhou, G. Z. Cheng, S. L. Chen and W. Luo, *ACS Catal.,* 2019, **9**, 3744-3752.
10. C. L. Hu, L. Zhang, Z. J. Zhao, A. Li, X. X. Chang and J. L. Gong, *Adv. Mater.,* 2018, **30**, 1705538.
11. H. J. Zhang, X. P. Li, A. Hähnel, V. Naumann, C. Lin, S. Azimi, S. L. Schweizer, A. W. Maijenburg and R. B. Wehrspohn, *Adv. Funct. Mater.,* 2018, **28**, 1706847.

Table S3. Comparison of the OER performance of Se-MnS/NiS with other recently reported electrocatalysts in 1 M KOH.

Catalyst	Electrolyte	Substrate	η_{10} (mV)	Tafel slope (mV dec^{-1})	Stability (h)	Reference
Se-MnS/NiS	1M KOH	Ni foam	211	55	48	This work.
MoS_2-Ni_3S_2 HNRs/NF	1M KOH	Ni foam	249	57	48	1
Co-Bi/BNC	1M KOH	Glassy carbon	286	70.9	20	2.
N-Fe_2PO_{5-x}-OT	1M KOH	Ni foam	235	27.2	30	3
Ni_2P-VP/NF	1M KOH	Ni foam	306	49	20	4
Co_9S_8/Ni_3S_2	1M KOH	Ni foam	227	46.5	9	5
w-$Ni(OH)_2$	1M KOH	Glassy carbon	237	33	12	6
CTGU-10c2	1M KOH	Glassy carbon	240	58	50	7
$Co(S_{0.22}Se_{0.78})_2$	1M KOH	Ni foam	283	65.6	20	8
NF/T(Ni_3S_2/MnS-O)	1M KOH	Ni foam	228	46	50	9
Ni_3Mn_1	1M KOH	Rotating disc electrode	260	44	16	10
FeOOH(Se)/IF	1M KOH	Iron foam	287	54	15	11

References

1. Y. Q. Yang, K. Zhang, H. L. Lin, X. Li, H. C. Chan, L. C. Yang and Q. S. Gao, *ACS Catal.,* 2017, **7**, 2357-2366.
2. Q. Hu, G. M. Li, Z. Han, Z. Y. Wang, X. W. Huang, X. Y. Chai, Q. L. Zhang, J. H. Liu and C. X. He,

Adv. Energy Mater., 2019, **9**. 1901130.

3. Y. Z. Wu, Y. N. Meng, J. G. Hou, S. Y. Cao, Z. M. Gao, Z. J. Wu and L. C. Sun, *Adv. Funct. Mater.,* 2018, **28**, 1801397.
4. H. J. Yan, Y. Xie, A. P. Wu, Z. C. Cai, L. Wang, C. G. Tian, X. M. Zhang and H. G. Fu, *Adv. Mater.,* 2019, **31**, 1901174.
5. F. Du, L. Shi, Y. T. Zhang, T. Li, J. L. Wang, G.H. Wen, A. Alsaedi, T. Hayat, Y. Zhou and Z. G. Zou, *Appl. Catal. B: Environ.,* 2019, **253**, 246-252.
6. J. Q. Yan, L. Q. Kong, Y. J. Ji, J. White, Y. Y. Li, J. Zhang, P. F. An, S. Z. Liu, S. T. Lee and T. Y. Ma, *Nat. Commun.,* 2019, **10**, 2149.
7. W. Zhou, D. D. Huang, Y. Pan. Wu, J. Zhao, T. Wu, J. Zhang, D. S. Li, C. H. Sun, P. Y. Feng and X. H. Bu, *Angew. Chem. Int. Ed.,* 2019, **58**, 4227-4231.
8. L. Fang, W. X. Li, Y. X. Guan, Y. Y. Feng, H. J. Zhang, S. L. Wang and Y. Wang, *Adv. Funct. Mater.,* 2017, **27**, 1701008.
9. Y. Zhang, J. L. Fu, H. Zhao, R. J. Jiang, F, Tian and R. J. Zhang, *Appl. Catal. B: Environ.,* 2019, **257**, 117899.
10. A. Sumboja, J. W. Chen, Y. Zong, P. S. Lee and Z. L. Liu, *Nanoscale*, 2017, **9**, 774-780.
11. S. Niu, W. J. Jiang, Z. X. Wei, T. Tang, J. M. Ma, J. S, Hu and L. J. Wan, *J. Am. Chem. Soc.,* 2019, **141**, 7005-7013.

Table S4. Comparison of the full water splitting performance of Se-MnS/NiS with other recently reported advanced electrocatalysts in 1 M KOH.

Catalyst	Electrolyte	Substrate	η_{10} (mV)	Stability (h)	Reference
Se-MnS/NiS	1 M KOH	Ni foam	1.47	48	This work.
Co-Bi/BNC	1 M KOH	Glassy carbon	1.53	20	1
NOGB-800	1 M KOH	Rotating disk electrode	1.65	20	2
Co@N-CS/N-HCP@CC	1 M KOH	Carbon cloth	1.545	24	3
Se-(NiCo)S/OH	1 M KOH	Ni foam	1.55	66	4
CoFe oxides/NF	1 M KOH	Ni foam	1.63	13.9	5
Ni_3N-VN/NF & Ni_2P-VP_2/NF	1 M KOH	Ni foam	1.51	100	6
NF/T(Ni_3S_2/MnS-O)	1 M KOH	Ni foam	1.54	50	7
NF-Ni_3S_2/MnO_2	1 M KOH	Ni foam	1.52	48	8
CoMoNiS-NF-31	1 M KOH	Ni foam	1.54	24	9
NiFeP/SG	1 M KOH	Rotating ring-disk electrode	1.54	40	10

References

1. Q. Hu, G. M. Li, Z. Han, Z. Y. Wang, X. W. Huang, X. Y. Chai, Q. L. Zhang, J. H. Liu and C. X. He, *Adv. Energy Mater.*, 2019, **9**. 1901130.

2. Q. Hu, G. M. Li, G. D. Li, X. F. Liu, B. Zhu, X. Y. Chai, Q. L. Zhang, J. H. Liu and C. X. He, *Adv. Energy Mater*., 2019, **9**, 1803867.
3. Z. L. Chen, Y. Ha, H. X. Jia, X. X. Yan, M. C, M. Liu and R. B. Wu, *Adv. Energy Mater*., 2019, **9**, 1803918.
4. C. L. Hu, L. Zhang, Z. J. Zhao, A. Li, X. X. Chang and J. L. Gong, *Adv. Mater.,* 2018, **30**, 1705538.
5. L. L. Huang, D. W. Chen, G. Luo, Y. R. Lu, C. Chen, Y. Q. Zou, C. L. Dong. Y. F. Li and S. Y. Wang, *Adv. Mater.,* 2019, **31**, 1901439.
6. H. J. Yan, Y. Xie, A. P. Wu, Z. C. Cai, L. Wang, C. G. Tian, X. M. Zhang and H. G. Fu, *Adv. Mater.,* 2019, **31**, 1901174.
7. Y. Zhang, J. L. Fu, H. Zhao, R. J. Jiang, F, Tian and R. J. Zhang, *Appl. Catal. B: Environ.,* 2019, **257**, 117899.
8. Y. Xiong, L. L. Xu, C. D. Jin and Q. F. Sun, *Appl. Catal. B: Environ.,* 2019, **254**, 329-338.
9. Y. Yang, H. Q. Yao, Z. H. Yu, S. M. Islam, H. Y. He, M. W. Yuan, Y. H. Yue, K. Xu, W. C. Hao, Gen. B. Sun, H. F. Li, S. L. Ma, P. Zapol and M. G. Kanatzidis, *J. Am. Chem. Soc.,* 2019, **141**, 10417-10430.
10. R. Q. Li, B. Lu. Wang, T. Gao, R. Zhang, C. Y. Xu, X. F. Jiang, J. J. Zeng, Y. Bando, P. F. Hu, Y. L. Li and X. B. Wang, *Nano Energy,* 2019, **58**, 870-876.